Published in final edited form as:

Adv Mater. 2014 May 28; 26(20): 3310–3314. doi:10.1002/adma.201306030.

Rapid Coating of Surfaces with Functionalized Nanoparticles for Regulation of Cell Behavior

Rui Tang,
Department of Chemistry, University of Massachusetts-Amherst, Amherst, Massachusetts, 01003, USA

Daniel F. Moyano,
Department of Chemistry, University of Massachusetts-Amherst, Amherst, Massachusetts, 01003, USA

Dr. Chandramouleeswaran Subramani,
Department of Chemistry, University of Massachusetts-Amherst, Amherst, Massachusetts, 01003, USA

Bo Yan,
Department of Chemistry, University of Massachusetts-Amherst, Amherst, Massachusetts, 01003, USA

Prof. Eunhee Jeoung,
Department of Chemistry, Gangneung-Wonju National University, Gangneung, Gangwon-do, 210-702, Korea

Gülen Yesilbag Tonga,
Department of Chemistry, University of Massachusetts-Amherst, Amherst, Massachusetts, 01003, USA

Bradley Duncan,
Department of Chemistry, University of Massachusetts-Amherst, Amherst, Massachusetts, 01003, USA

Yi-Cheun Yeh,
Department of Chemistry, University of Massachusetts-Amherst, Amherst, Massachusetts, 01003, USA

Ziwen Jiang,
Department of Chemistry, University of Massachusetts-Amherst, Amherst, Massachusetts, 01003, USA

Dr. Chaekyu Kim, and
Department of Chemistry, University of Massachusetts-Amherst, Amherst, Massachusetts, 01003, USA

Prof. Vincent M. Rotello

Correspondence to: Vincent M. Rotello, rotello@chem.umass.edu.

Supporting Information is available online from Wiley InterScience or from the author.

Department of Chemistry, University of Massachusetts-Amherst, Amherst, Massachusetts, 01003, USA

Vincent M. Rotello: rotello@chem.umass.edu

Keywords

Surface modification; nanoparticle; cell regulation; nanomanufacturing

Material properties such as surface morphology,[1] chemistry,[2] hydrophobicity,[3] and elasticity[4] can be used to regulate cell growth. With proper surface modification, cells can grow on materials otherwise biologically incompatible including plastics and inorganic platforms, such as polyester, polycaprolactone, polyetheretherketone, alumina and calcium phosphate.[5] These modified surfaces have been used for *in vitro* cell culture, [6] tissue regeneration and organ rebuilding.[7] Selectivity of cell proliferation on surfaces is an additional requirement for multiple applications, including wound healing,[8] tissue repair,[9] and cellular applications including cell residence, development, and differentiation.[10] The capability of such surfaces to dictate cellular fate can be obtained by precisely defining surface components and structures. For example, RGD peptide has been used to selectively stimulate specific cell growth.[11] Topography has also been harnessed to selectively trigger cell fate decisions.[12]

Specifically tailoring surfaces to support growth of specific cell types is challenging, particularly in the context of processes amenable to manufacturing.[13] While cells respond to their supporting microenvironment,[14] developing a general strategy for precisely tuning the surface to optimize biocompatibility of specific cell type is challenging. Issue to be addressed include identifying appropriate surfaces, while manufacturing is complicated by the use of complex coating processes such as layer-by-layer deposition[15] and nanopatterning[16] that are costly and time consuming and therefore challenging to implement for large-scale production.

Herein, we describe a rapid and scalable strategy to deposit a thin coating (~ monolayer) of functionalized gold nanoparticles (AuNPs) onto commercial polystyrene cell-culture plates. By tuning the terminal group of the ligand, the properties of AuNPs and hence the resulting surface properties can be precisely modulated to regulate cellular behavior. This control of surface functionality yields surfaces that show cell type selectivity in cell viability.

The first step for our modulation strategy is the “painting” of the surfaces using AuNPs. For our studies, AuNPs with 2 nm cores were functionalized with a variety of surface ligands. These ligands were designed to prevent protein fouling, maximizing the role of the particle in dictating cellular interactions.[7] In our previous approach to NP-mediated surface modification, AuNPs with defined ligands were immobilized onto surfaces through chemical crosslinking.[18] However, this method requires extra steps. In addition, the crosslinking reagents are cytotoxic and the residual after the reaction cannot be completely removed. In the current approach particles were deposited through simple dip coating of the particles in an aqueous solution onto commercial plasma-oxidized polystyrene cell-culture plates. (Figure 1a). Interactions between the plate and the AuNPs provided irreversible particle

deposition (*vide infra*). The process was also self-passivating: after formation of an AuNP monolayer, no extended deposition onto the surface was observed due to electrostatic repulsion between particles.

A TTMA AuNP layer (Figure 1a) was generated to as a prototype the AuNP-modified surfaces. The AuNP layer was formed by dipping a plasma-treated polystyrene culture plate surface into 100 nM aqueous solution of TTMA AuNPs. No significant differences in surface morphology and roughness between untreated and TTMA AuNP coated surfaces were observed (Figure S1) as detected by Atomic Force Microscopy (AFM). The AuNP layer on the template was then characterized by depth profiling using angle-resolved X-ray photoelectron spectroscopy (XPS).[19] As shown in Figure 1b, there was a strong angular dependence of the Au peak and other peaks associated with the AuNP signal. Particularly, the C/Au ratio increased from 45 (15°) to 91 (75°) with increasing take-off angle. This angle-dependent increase coupled with the shake-up peak from the π-π interaction of polystyrene observed at 75° (inset of Figure 1b), confirms the detection of the polystyrene substrate. Considering the detection depth of XPS is *ca.* 5 nm,[20] the thickness of the AuNP layer can be estimated to be less than 5 nm, consistent with a monolayer of particles.

The TTMA AuNP film was robust under cell-culture conditions: after washing with phosphate buffered saline (PBS) three times, the surface was incubated with Dulbecco's Modified Eagle Medium (DMEM) containing 10% serum at 37 °C for 24 h, followed by treatment with trypsin for 5 min. After this treatment, the loss of the AuNPs from the surface was negligible, as determined by inductively-coupled plasma mass spectrometry (ICP-MS) (Figure 1c). Even after one week of culture replacing the media every other day, minimal AuNP leaching was detected, while a substantial amount of AuNPs (86.7%) remained in the plate (Figure S2). In contrast, without plasma treatment, TTMA AuNPs were easily washed away indicating that plasma treatment of the polystyrene surface is essential for creation of a stable monolayer of AuNPs.

Preliminary insight into the interaction of particle-modified surfaces and cells was obtained using surfaces coated with TTMA AuNPs. HepG2 cells were grown in the cell-culture plates with or without a TTMA AuNP coating. After 80 min incubation, cells cultured on the TTMA AuNP treated surface have already adhered, with and filopodia starting to form. In contrast, very few cells attached to the plate surface without AuNP layer at the same time point (Figure S3). After 24 h incubation, cells cultured on the TTMA AuNP treated surface exhibit distinctly different morphologies, with TTMA-treated surfaces encouraging cell spreading relative to the untreated control (Figure 2 and Figure S4). Staining with phallotoxin to specifically target F-actin demonstrates that cells grown on the AuNP surface have more filopodia than those grown on a plasma-treated surface (Figure 2c–d, Figure S5), indicative of enhanced adhesion.[21] Taken together, these results reveal that TTMA AuNP monolayers can be successfully used to enhance the adhesion of cells. It is notable that ICP-MS indicated no loss of AuNPs from the polystyrene surface (Figure 2e), despite the fact that positively charged nanoparticles are known to be readily taken up by cells.[22] Substitution of the AuNP for a TTMA CdSe quantum dot (core diameter ≈ 3 nm) also showed a stimulatory effect on cell morphogenesis that resembled that of the TTMA AuNPs

(Figure S6). Thus it is clear that it is the surface ligand, rather than the core of the nanoparticle, that plays an important role in regulating the cell behavior.

Variation of surface ligands on AuNPs can be used to control surface properties, [23] providing a potential tool to regulate cellular behavior. To test this hypothesis, the effects of AuNP coatings on the viability on four kinds of cells from different organs was determined, namely HepG2 (human liver), HeLa (human cervix), MCF7 (human breast), and 3T3 (murine fibroblast). To perform this study, 26 kinds of functionalized AuNPs were screened, with different types of ligands of varying hydrophobic, stereoelectronic, constitutional, and aromatic characteristics (Figure 3).

Cell viability was determined using an Alamar blue assay (Figure 3). The matrix of the 26 nanoparticles against the four cell lines indicated that different AuNPs had marked and selective effects on the viability of the different cell lines. It is evident that these cationic NPs (TTMA) dramatically increased the viability of HepG2 cells and to a lesser extent MCF7 cells, while having minimal effect on HeLa and 3T3 cells. These differences among cell types arise due to the sensitivity of the cells responding to the environment. However, this tendency was not universal and certain cationic nanoparticles promoted the growth of specific cell lines while inhibiting others, for example aromatic functionalities (T-Ph and T-Benzyl) that significantly boosted the viability of HepG2 comparative to the other the cell lines. A similar case was observed when the hydrophobicity of the ligand increases. While the more hydrophilic NPs (TTMA to T-C6, and T-C2-NH2 to T-C3-OH2) boosted the viability of both HepG2 and MCF7, the more hydrophobic NPs (T-C14 to T-dbC6) increased the viability only for HepG2, as MCF7 is apparently more sensitive to the cytotoxic properties of the hydrophobic moieties.

Constitutional isomerism has a significant effect on the viability pattern of the cells, with T-cyC6 inhibiting the growth of MCF7 while increasing HeLa and 3T3 viability, contrasting with T-C6 that only boosted the growth of MCF7. On the other hand, the stereoisomeric nature of the terminal group had little effect on the preferential cell viability, as demonstrated by comparing the cases of the two T-Phe NPs (L and D), as well as the three different sugar functionalized NPs (T-Glu, T-Man and T-Gal). This observation was surprising, as a dissimilar behavior was expected to arise from the different levels of specific receptors at the surfaces of the cells, *e.g.*, HepG2 cell contains galactose receptor while HeLa cell does not.[24] It is important to note that despite the fact that the surface coverage with the AuNPs varied somewhat between the particles, there is no significant correlation between coverage the observed changes in cell viability (Figure S8), strengthening our hypothesis that the is the principle factor controling cell behavior.

In conclusion, we developed a facile strategy to generate robust surfaces coated with AuNP monolayers. As shown by our preliminary studies, the surfaces are tunable in an “atom-by-atom” fashion, allowing the exploration of a wide variety of surface chemistries. The ability to foster the selective growth of specific cell types makes these surfaces promising for medical applications such as wound healing and transplantation. Finally, the ready scalability of the deposition process makes these surfaces attractive for real-world manufacturing.

Experimental

AuNP coating

AuNPs were dissolved in MilliQ water at a concentration of 100 nM prior to coating. Then 500 μL of AuNP solution were incubated in one well of a 24-well plate at 37 °C for 3 h (125 μL for 96-well plate). Excess AuNPs were washed away with water three times followed by complete drying at 37 °C.

Characterizations

For both AFM and XPS characterization, the bottom of the plate coated by AuNPs was carefully removed. AFM imaging was performed on a DI Dimension-3100 AFM. Both height and phase images were collected. The average roughness of the determined sample area was calculated by Gwyddion, a freeware with the agreement of GNU General Public License. XPS analysis was performed on a Physical Electronics Quantum 2000 spectrometer using a monochromatic Al Kα excitation at a spot size of 10 mm with pass energy of 46.95 eV at take-off angles of 15°, 45°, and 75°. For stability testing, the TTMA AuNP coating process was performed on a 96-well plate with or without plasma treatment. After washing with PBS three times, the surface was incubated with DMEM media containing 10% serum at 37 °C for 24 h, followed by treatment with trypsin for 5 min. AuNPs left on the plates were dissolved by using *aqua regia* for inductively coupled plasma mass spectrometry detection.

Cell culture

Cells were cultured in a humidified atmosphere (5% CO_2) at 37 °C, and grown in Dulbecco's Modified Eagle's Medium (DMEM, low glucose) supplemented with 10% fetal bovine serum (FBS) and 1% antibiotics (100 U/mL penicillin and 100 μg/mL streptomycin). To culture cells on the plates, 30,000 or 7,500 cells were plated on 24- or 96-well plates for a desired time (80 min, 24 h or one week), respectively.

Cell viability assay

7,500 cells were cultured in a 96-well plate for 24 h with or without AuNP coating. Cells were then incubated with 200 μL DMEM containing 10% Alamar Blue. Cells growing in untreated wells were set as "Blank" group. The "Untreated" group was set by adding the same volume of the Alamar Blue media into the untreated wells without cells. After 3 h incubation, the fluorescence intensity (FI) of reduced Alamar Blue at 590 nm from each well was recorded with an excitation wavelength of 535 nm. By defining the cell viability of Blank as 100%, the viabilities of cells growing on AuNP coated wells were calculated using the following equation:

$$Cell\ viability\,\%=FI-FI\ Untreated\ FI\ Blank-FI\ Untreated\times 100\%$$

Where FI_{Blank} is the average fluorescence intensity of "Blank" group and $FI_{untreated}$ is the average fluorescence intensity of "Untreated" group.

Supplementary Material

Refer to Web version on PubMed Central for supplementary material.

Acknowledgments

This research was supported by the NIH (GM077173) and the NSF (NSEC (CMMI-1025020) and MRSEC(DMR-0820506))

References

1. Qi L, Li N, Huang R, Song Q, Wang L, Zhang Q, Su R, Kong T, Tang M, Cheng G. PLoS One. 2013; 8:e59022. [PubMed: 23527077]
2. a) Zheng W, Zhang W, Jiang X. Adv Healthcare Mater. 2013; 2:95.b) Mrksich M. Chem Soc Rev. 2000; 29:267.
3. a) Valamehr B, Jonas SJ, Polleux J, Qiao R, Guo S, Gschweng EH, Stiles B, Kam K, Luo TJM, Witte ON, Liu X, Dunn B, Wu H. Proc Natl Acad Sci U S A. 2008; 105:14459. [PubMed: 18791068] b) Arima Y, Iwata H. Biomaterials. 2007; 28:3074. [PubMed: 17428532]
4. a) Skardal A, Mack D, Atala A, Soker S. J Mech Behav Biomed Mater. 2013; 17:307. [PubMed: 23122714] b) Kawano T, Nakamichi Y, Fujinami S, Nakajima K, Yabu H, Shimomura M. Biomacromolecules. 2013; 14:1208. [PubMed: 23510479]
5. a) Jiao YP, Cui FZ. Biomed Mater. 2007; 2:R24. [PubMed: 18458475] b) Ma Z, Mao Z, Gao C. Colloids and Surfaces B: Biointerfaces. 2007; 60:137.c) Bertazzo S, Zambuzzi WF, da Silva HA, Ferreira CV, Bertran CA. Clin Oral Implant Res. 2009; 20:288.d) Roohani-Esfahani SI, Nouri-Khorasani S, Lu ZF, Fathi MH, Razavi M, Appleyard RC, Zreiqat H. Mater Sci Eng C-Mater Biol Appl. 2012; 32:830.Lee JH, Jang HL, Lee KM, Baek HR, Jin K, Hong KS, Noh JH, Lee HK. Acta Biomater. 2013; 9:6177. [PubMed: 23212079]
6. Mazia D, Schatten G, Sale W. J Cell Biol. 1975; 66:198. [PubMed: 1095595]
7. a) Meese TM, Hu YH, Nowak RW, Marra KG. J Biomater Sci-Polym Ed. 2002; 13:141. [PubMed: 12022746] b) Da Silva RMP, Mano JF, Reis RL. Trends Biotechnol. 2007; 25:577. [PubMed: 17997178] c) Sipehia R, Martucci G, Lipscombe J. Artif Cell Blood Sub. 1996; 24:51.
8. Stanford CM. Int J Mol Sci. 2010; 11:354. [PubMed: 20162020]
9. Garcia JL, Asadinezhad A, Pachernik J, Lehocky M, Junkar I, Humpolicek P, Saha P, Valasek P. Molecules. 2010; 15:2845. [PubMed: 20428083]
10. a) Li N, Zhang X, Song Q, Su R, Zhang Q, Kong T, Liu L, Jin G, Tang M, Cheng G. Biomaterials. 2011; 32:9374. [PubMed: 21903256] b) Phillips JE, Petrie TA, Creighton FP, Garcia AJ. Acta Biomater. 2010; 6:12. [PubMed: 19632360]
11. Hersel U, Dahmen C, Kessler H. Biomaterials. 2003; 24:4385. [PubMed: 12922151]
12. Engel Y, Schiffman JD, Goddard JM, Rotello VM. Mater Today. 2012; 15:478.
13. Variola F, Brunski JB, Orsini G, Tambasco de Oliveira P, Wazen R, Nanci A. Nanoscale. 2011; 3:335. [PubMed: 20976359]
14. Berg, JM.; Tymoczko, JL.; Stryer, L. Biochemistry. W H Freeman; New York: 2002.
15. a) Lee H, Jang Y, Seo J, Nam JM, Char K. ACS Nano. 2011; 5:5444. [PubMed: 21702475] b) Fukuda J, Khademhosseini A, Yeh J, Eng G, Cheng J, Farokhzad OC, Langer R. Biomaterials. 2006; 27:1479. [PubMed: 16242769]
16. Bacakova L, Filova E, Parizek M, Ruml T, Svorcik V. Biotechnol Adv. 2011; 29:739. [PubMed: 21821113]
17. Moyano DF, Rotello VM. Langmuir. 2011; 27:10376. [PubMed: 21476507]
18. Park MH, Subramani C, Rana S, Rotello VM. Adv Mater. 2012; 24:5862. [PubMed: 22915042]
19. Wen J, Somorjai G, Lim F, Ward R. Macromolecules. 1997; 30:7206.
20. Barr, TL. Modern ESCA: the Principles and Practice of X-Ray Photoelectron Spectroscopy. CRC Press; Boca Raton: 1994. p. 75

21. a) Schäfer C, Borm B, Born S, Möhl C, Eibl EM, Hoffmann B. Exp Cell Res. 2009; 315:1212. [PubMed: 19100734] b) Tsui HC, Lankford KL, Klein WL. Proc Natl Acad Sci U S A. 1985; 82:8256. [PubMed: 3865227]

22. Zhu ZJ, Carboni R, Quercio MJ, Yan B, Miranda OR, Anderton DL, Arcaro KF, Rotello VM, Vachet RW. Small. 2010; 6:2261. [PubMed: 20842664]

23. Subramani C, Saha K, Creran B, Bajaj A, Moyano DF, Wang H, Rotello VM. Small. 2012; 8:1209. [PubMed: 22354857]

24. Satoh T, Kakimoto S, Kano H, Nakatani M, Shinkai S, Nagasaki T. Carbohydr Res. 2007; 342:1427. [PubMed: 17548066]

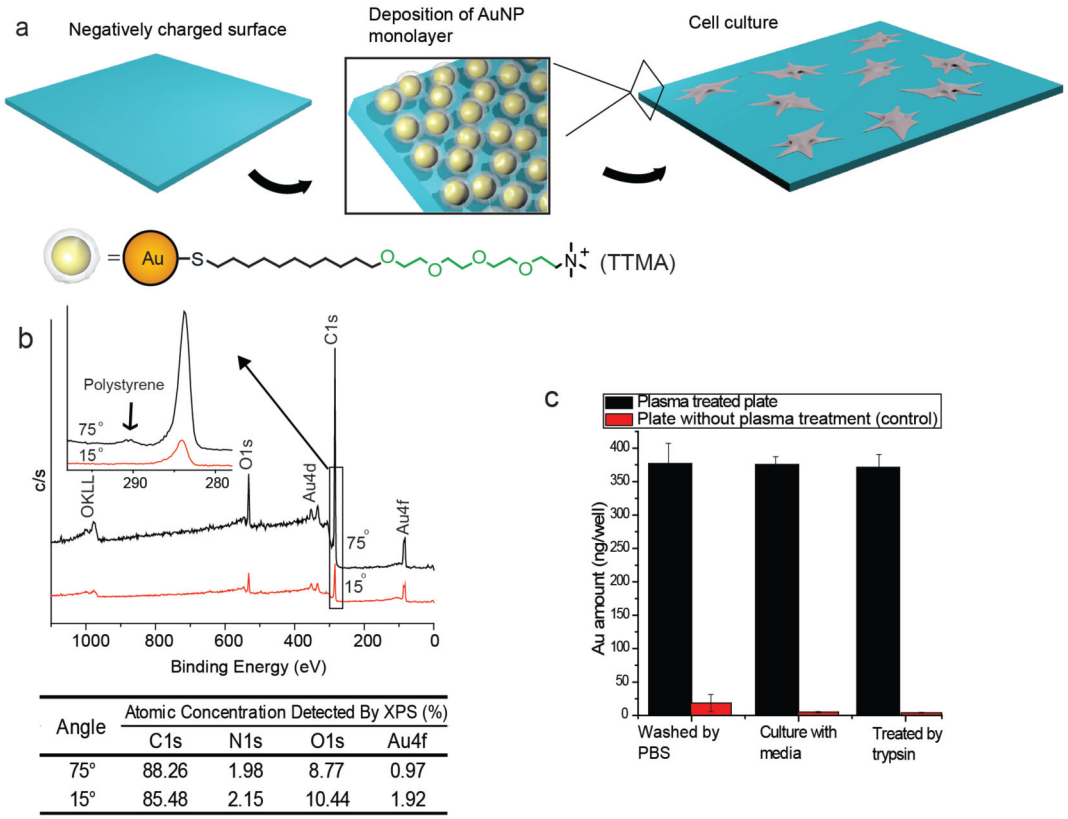

Angle	Atomic Concentration Detected By XPS (%)			
	C1s	N1s	O1s	Au4f
75°	88.26	1.98	8.77	0.97
15°	85.48	2.15	10.44	1.92

Figure 1.

Preparation and characterization of TTMA AuNP layer on the polystyrene-plate surface. a) Schematic representation of the strategy to generate a AuNP monolayer on the cell-culture plate. b) Angle-resolved XPS detection of the polystyrene-plate surface with the AuNP layer. Relative atomic concentrations of C, N, O and Au are listed in the table. c) AuNPs attached to the plate with or without plasma treatment under cell-culture conditions. Each bar represents the amount of gold left in one well of a 96-well plate. The error bars represent the standard deviation of three measurements.

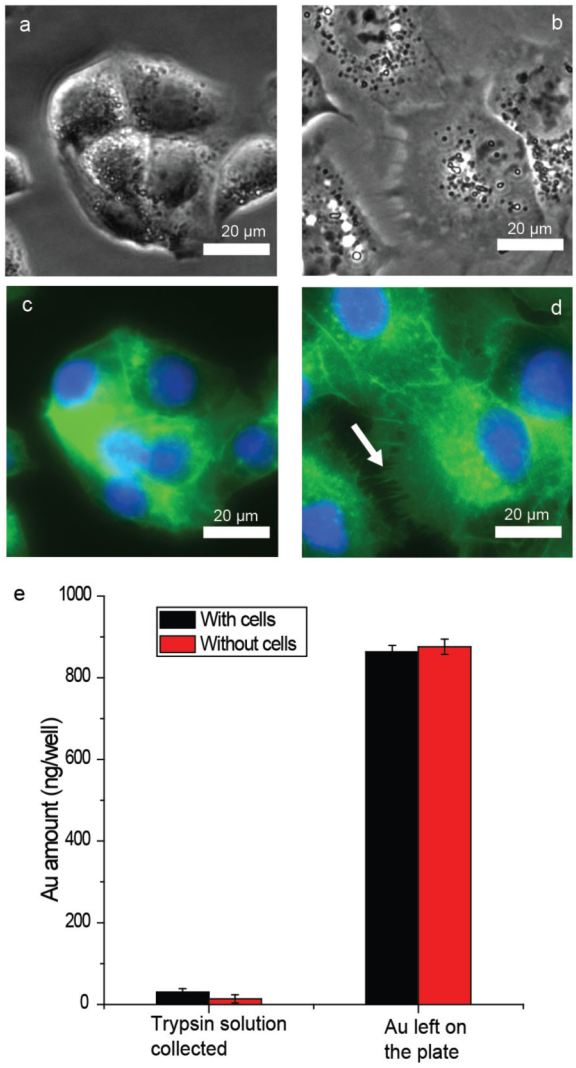

Figure 2.

HepG2 cell culture for 24 h on plates with and without the TTMA AuNP layer. a) Optical image of HepG2 cell grown on a plasma-treated plate. b) Optical image of HepG2 cell grown on a TTMA AuNP monolayer. c) Fluorescent image of Figure 2a. F-actin was stained by Oregon Green labeled phallotoxin, and the nuclei were stained by Hoechst 33342. d) Fluorescent image of Figure 2b. The staining conditions were the same as in Figure 2c. The arrow indicates filopodia of the cell. Separated fluorescent channels of Figure 2c and d can be seen in Figure S5. e) Cell-uptake test of TTMA AuNP monolayer. The cells were cultured on the TTMA AuNP monolayer in a 24-well plate for 24 h. A 24-well plate coated with TTMA AuNPs without cells cultured on the surface was used as a control.

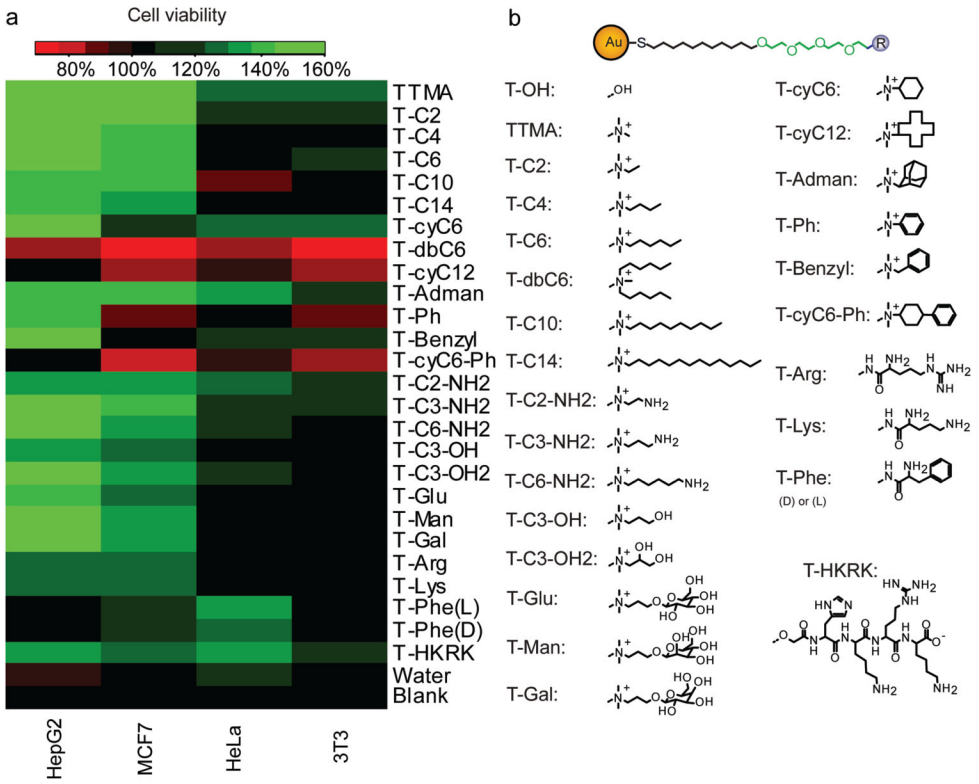

Figure 3.

Cell viability assay for 26 different AuNP coatings (morphology changes of HepG2 cell were shown in Figure S7). a) A heat map of cell viability influenced by different AuNP coatings. b) Structures of ligands on the AuNPs. ‘Blank’ represents the cell viability on plasma-treated surface without any pretreatment, and ‘Water’ represents the cell viability on the surface pretreated with water only (no AuNP added) for 3 h and without post deposition of AuNPs.